Application of Piezofilms for Excitation and Active Damping of Blade Flexural Vibration

Luděk PEŠEK, Ladislav PŮST, Vítězslav BULA, Jan CIBULKA

Institute of Thermomechanics AS CR, v.v.i.
Dolejškova 5, 18200 Praha 8, Czech Republic; e-mail: pesek@it.cas.cz

The steam turbine blades of low pressure stages are endangerd by the high-cyclic fatigue due to the combined loading of dynamic stresses by the steam time-variant pressure and the pre-stress from centrifugal forces. Therefore, the importance of their experimental dynamic analysis in the design stage is critical. For laboratory tests of the blades, the piezo actuators placed on the blades, unlike electromagnets placed in the stationary space, give a possibility to excite the flexural vibration of the blades within the bladed disk by time continuous forces independently of the rotor revolutions. In addition, the piezo actuators can be also used to control the vibrations of the blade. Therefore, several dynamic experiments of the clamped model blade equipped with PVDF films were performed for the force description of the piezo foils and their behavior as actuators of the blade vibration. The numerical beam models were used for numerical analysis of the vibration suppression effects both by additional parametric excitation and by active damping. The optimal phase shift of piezo actuator voltage supply was ascertained both for amplitude amplification and suppression. The results contribute to the knowledge of the actuation and active damping of blade vibration by the piezo elements.

Keywords: vibration suppression, parametric antiresonance, active damping, PVDF films.

1. Introduction

The dynamic behavior of bladed discs was investigated in our structural dynamic laboratory (PEŠEK *et al.*, 2012; PŮST, PEŠEK, 2011). The major attention is drawn to the bladed models with inter-blade dry friction couplings and models with additional elements of high damping materials. Their behavior is dependent on excitation amplitudes due to material and structural non-linearities. Therefore, the proper actuations of the resonant vibration under rotation are still under development. Electromagnets as the dynamic actuators are placed on the stator part against the blade tips and their impulses are synchronized with the wheel revolution. However, this type of excitation is revolution conditioned since it is necessary to set a so-called critical revolutions of the wheel to excite its resonant vibration (PEŠEK *et al.*, 2010; 2011).

The polyvinylidene fluoride (PVDF) film and PZT patch transducers give the possibility to excite the vibration of the thin structures by direct coupling to the structure (PREUMONT, 2011; AUGUSTYN, 2014; NADER, 2013). It would enable to excite the resonant vibration of blades by time-continuous forces independently of the revolutions. However, using this principle of blade excitation is conditioned – besides the resistivity to severe conditions of rotational tests – by demands of their sufficient mechanical power and also for the identification and control purposes by a calibratable force effect. Furthermore, the piezoelectric foils could be used as the actuators for the vibration control, e.g. suppression of dangerous blade vibrations.

Therefore, the experiment of the clamped model blade excited by the two strips of PVDF film was prepared. Besides the piezo actuators, the electromagnet as the reference source of excitation was installed at the end of the blade. The experiments with only PVDF actuators helped evaluate the values of bending moments of the piezoelectric strips.

For analysis of suppression of the forced resonant vibration, the optimal phase angle of piezo actuator input time signal with respect to the electromagnet input time signal was ascertained experimentally. Besides the usage of PVDF films by active damping (NORDMAN, 2005; WARMINSKI *et al.*, 2011; 2013; JARZYNA *et al.*, 2012), the paper deals with possibilities of an application of the additional parametric excitation (TONDL, PŮST, 2012; PEŠEK, TONDL, 2012; TŮMA *et al.*, 2014)

as a tool for the suppression of the blade vibration. By adding the parametric excitation, the equations of motion are governed by linear differential equations with periodic timevariable coefficients. It is well known that these systems can be unstable in the vicinity of the first kind resonance and combination resonance frequencies. The combination resonances can be additive or subtractive. It was, however, discovered and mathematically proven (TONDL, 1998) that the excitation by combination subtractive resonance frequency brings stabilization and suppression effects into self-excited and externally excited vibrations under single harmonic excitations. Since the bladed wheels suffer especially by dominant resonant vibrations (PEŠEK *et al.*, 2014a), we decided to deal with this technique for its suppression.

2. Force actuation of the piezoelectric film

The electrical field acting between the electrodes of elements of piezoelectric materials causes their dimensional changes. The sizes of these changes are given by the piezoelectric constants of the material. Suppression of some of these changes leads to a force actuation on the body in contact with piezomaterial by the blocking force F_B (BELL, 1993). In case when thin piezoelectric layers are glued on the beam (see Fig. 1) the blocking force evokes bending moments M_p acting against each other on the more distant ends of the strip (PREUMONT, 2011)

$$M_p = -F_B z_m = -E_p d_{31} U b_p z_m, \qquad (1)$$

where E_p is the Young modulus of piezomaterial, d_{31} [m/V] is the piezoelectric constant between axis 3 (direction of longitudinal axis of the strip) and axis 1 (direction perpendicular to the strip plane), U [V] supply voltage, b_p width of the strip, z_m distance of the neutral axis of the beam from the plane of the piezolayer.
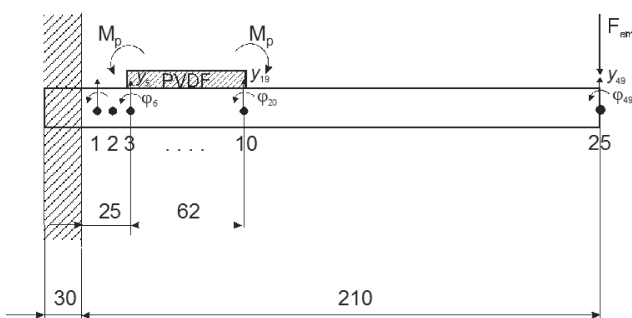

Fig. 1. Chart of the beam FE model with the one-side PVDF film layout.

For indirect evaluation of the bending moments from the experimental ascertained resonant amplitudes of the clamped beam vibration, the finite element beam model consists of 25 elements and is based on the Euler theory. Each node $i = 1, 2, .., 25$ of the FE model has two degrees of freedom (DOF), i.e. a transversal displacement y and an angular displacement φ indexed by $2 \cdot i - 1$ and $2 \cdot i$, respectively, in the global displacement vector of the beam.

The evaluation of the bending moments M_p of the piezo actuator acting on the corresponding DOFs φ_6, φ_{20} of the model is presented in (PEŠEK *et al.*, 2014b).

3. Numerical simulations of a forced resonance vibration suppressed by additional parametric excitation

The parametric "anti-resonance" effect (TONDL, PŮST, 2012) for suppression of a forced resonant vibration by additional parametric excitation is studied in this paper on the numerical simulation. We came from the equation of motion of the finite element beam model (Fig. 1)

$$(\mathbf{K} + \varepsilon \mathbf{K}_p \cos(\nu t))\mathbf{y}(t) + \mathbf{B}\dot{\mathbf{y}}(t) + \mathbf{M}\ddot{\mathbf{y}}(t) = \mathbf{f}_b(t), \quad (2)$$

where $\mathbf{K}$, $\mathbf{B}$ and $\mathbf{M}$ are stiffness, damping and mass matrices; $\mathbf{y}$, $\dot{\mathbf{y}}$ and $\ddot{\mathbf{y}}$ are the vectors of displacement, velocity and acceleration, respectively. Vector $\mathbf{f}_b$ represents force vector. Matrix $\mathbf{K}_p$ is multiplied by the small parameter ε and by the function $\cos(\nu t)$ represents parametric excitation contribution periodically variable with frequency ν. The structure of the matrix $\mathbf{K}_p$ was composed from the zeros matrix of the same dimensions as $\mathbf{K}$ with imposed diagonal angular displacement beam stiffness – $k_{6,6}$ and $k_{20,20}$ at nodes 3 and 10, respectively. Multiplying of these components by the corresponding angular displacements gives the bending moments $M_{p,3}$ and $M_{p,10}$ by PVDF films at these nodes.

Assuming the weak influence of the parametric excitation on the modal behavior of the blade and stiffness proportional damping, we transform the Eq. (2) into the so-called quasi-normal model

$$(\mathbf{k}_R + \varepsilon \mathbf{k}_{pR}(\cos(\nu t)))\mathbf{y}_R + \beta \mathbf{k}_R \dot{\mathbf{y}}_R + \mathbf{m}_R \ddot{\mathbf{y}}_R = \mathbf{f}_{bR}, \quad (3)$$

where $\mathbf{y} = \mathbf{X}\mathbf{y}_R$, $\mathbf{k}_{pR} = {}^T\mathbf{X}\mathbf{K}\mathbf{X}$, $\mathbf{k}_R = {}^T\mathbf{X}\mathbf{K}_p\mathbf{X}$, $\mathbf{m}_R = {}^T\mathbf{X}\mathbf{M}\mathbf{X}$, $\mathbf{f}_{bR} = {}^T\mathbf{X}\mathbf{f}_b$ and β is stiffness coefficient of proportional damping. The letter $\mathbf{X}$ represents a modal matrix.

If the modal matrix consisted of the first two eigenmodes $\mathbf{X} = [\mathbf{x}_1, \mathbf{x}_2]$ is orthonormalized to the mass matrix $\mathbf{M}$, then we can simplify the Eq. (3) into

$$\begin{bmatrix} \ddot{y}_{1R} \\ \ddot{y}_{2R} \end{bmatrix} = -\left(\begin{bmatrix} \Omega_1^2 & 0 \\ 0 & \Omega_2^2 \end{bmatrix} \begin{bmatrix} y_{1R} \\ y_{2R} \end{bmatrix} \right.$$

$$+ \varepsilon \cos(\nu t) \begin{bmatrix} k_{pR11} & k_{pR12} \\ k_{pR21} & k_{pR22} \end{bmatrix} \begin{bmatrix} y_{1R} \\ y_{2R} \end{bmatrix}$$

$$\left. + \beta \begin{bmatrix} \Omega_1^2 & 0 \\ 0 & \Omega_2^2 \end{bmatrix} \begin{bmatrix} \dot{y}_{1R} \\ \dot{y}_{2R} \end{bmatrix} - \begin{bmatrix} f_{bR1} \\ f_{br2} \end{bmatrix} \right). \quad (4)$$

The solution of the Eq. (4) was ascertained by the Runge-Kutta method of the fourth order. The computed parameters of the Eq. (4) for FE model (Fig. 1) of the steel beam (heigh : width : length = $10 \times 18 \times 240$ mm) subjected to the force $F_{em} = 1$ N were: $\Omega_1 = 1082.9$, $\Omega_2 = 6745.2$, $\beta = 8e{-}4$ (material damping ratio 0.08%), $f_{bR1} = 0.3399$, $f_{bR2} = 0.3382$, $k_{pR11} = 1.0378e7$, $k_{pR12} = k_{pR21} = 1.1239e7$, $k_{pR12} = -7.9801e7$.

The parametric antiresonance frequency $\nu = \Omega_2 - \Omega_1 = 5662.3$ (TONDL, 1998) was chosen for the parametric excitation.

The time characteristics of displacements at the end y_{49} and middle y_{23} of the blade during a slow sweep excitation frequency rate ($\mathrm{d}\omega/\mathrm{d}t = 0.2$ rad/s^2) in the vicinity of the frequency $\omega = \langle 1080.7, 1086.4 \rangle$ rad/s are shown without ($\varepsilon = 0$) and with ($\varepsilon = 1e^{-2}$) para-

metric excitation in Fig. 2. The time characteristics of Fig. 2 zoomed in the vicinity of the first eigenfrequency Ω_1 are drawn in Fig. 3. Besides the displacements, the characteristics of both excitations, i.e. force F_{em} (solid line) and parametric excitation scaled to a unit amplitude (dashed line), are also depicted on the bottom of Fig. 3. Comparing amplitudes of y_{49} and y_{23} with and without the additional parametric excitation proves the theoretical assumption of the influence of the parametric antiresonance: the forced vibration is lowered due to increased damping by the antiresonance. The damping effect increases with the increase of the amplification parameter ε. The zoom characteristics (Fig. 3) show the origination of modulation of the force excited displacements by the second resonant frequency due to the parametric excitation.
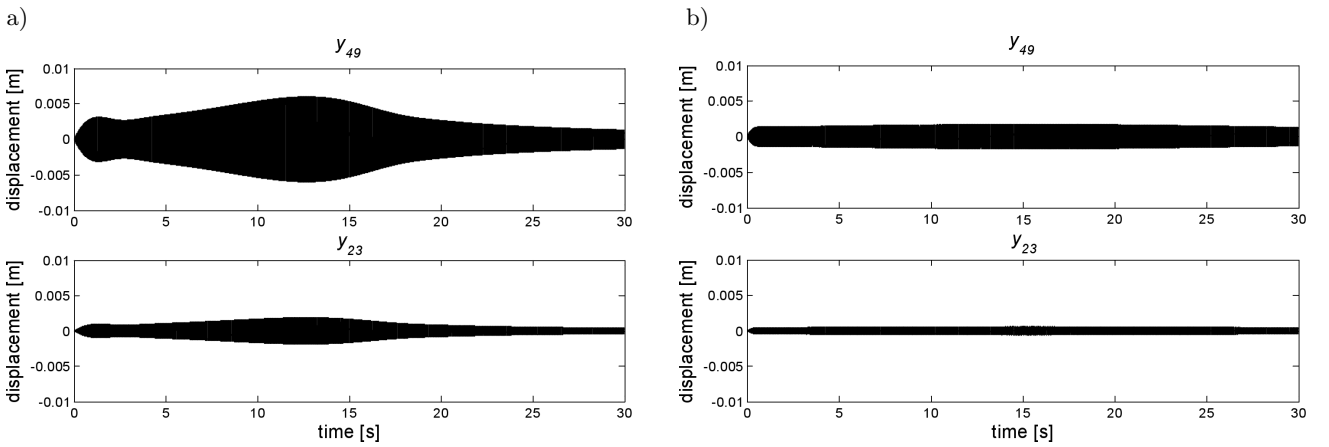
a)

b)

Fig. 2. Time characteristics of displacements at the end y_{49} (top) and middle y_{23} (bottom) of the blade during a slow sweep excitation frequency rate in the frequency range $\omega = \langle 1080.7, 1086.4 \rangle$ rad/s: a) without additional parametric excitation ($\varepsilon = 0$), b) with additional parametric excitation ($\varepsilon = 1e^{-2}$).
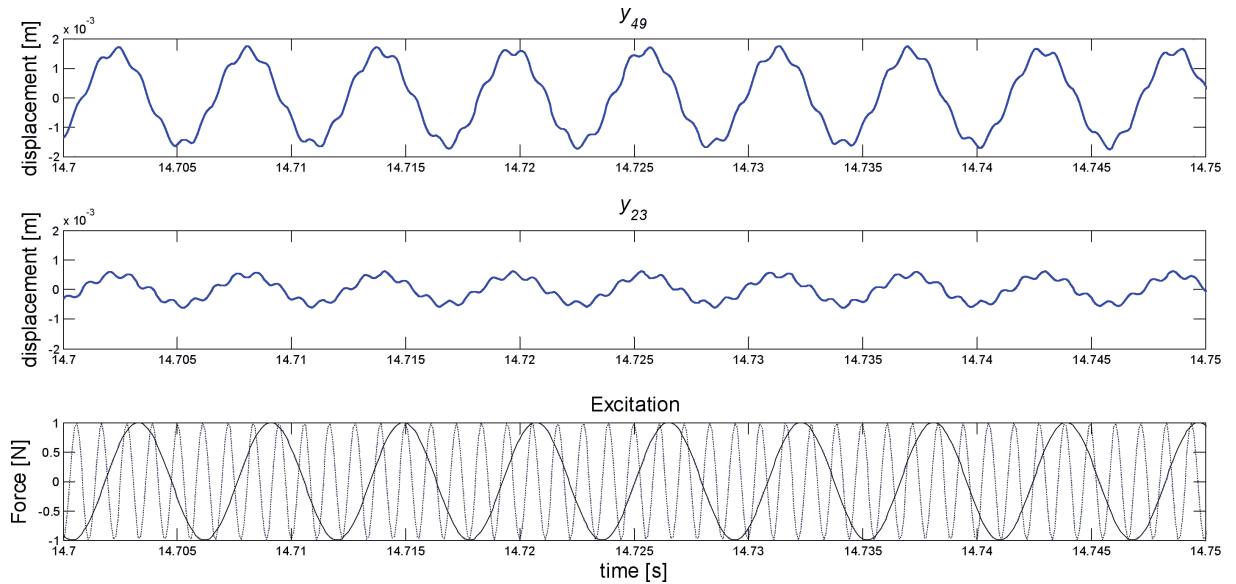

Fig. 3. The time characteristics of displacements y_{49} (top), y_{23} (middle) of the blade and of force (solid) and parametric (dashed line) excitations (bottom) under a slow sweep excitation frequency rate ($\mathrm{d}\omega/\mathrm{d}t = 0.2$ rad/s^2) zoomed in the vicinity of first eigenfrequency $\Omega = 1037.8$ rad/s and additional excitation ($\varepsilon = 1e^{-2}$).

4. Numerical simulations of the forced resonance vibration suppressed by active damping

Active damping is often applied to reduce oscillations in the aeronautic apparatus (RYBAK, 1997), where other types, e.g. hydraulic, cannot be used. However, the same principle is also applicable in machinery

A damped element, e.g. a turbine blade, has to be provided by two transducers: a sensor S_1 picking up displacement $x(t)$ and generating a signal feeding after adaptation, and amplification actuator S_2 producing force proportional to the velocity $\dot{x}(t)$. A signal proportional to the displacement $x(t)$ is transformed into a signal similar to velocity in the feedback loop, i.e. amplified with phase shift $\approx \pi/2$ and then introduced as a damping force signal back into the actuator producing additional damping force in the controlled dynamical system.
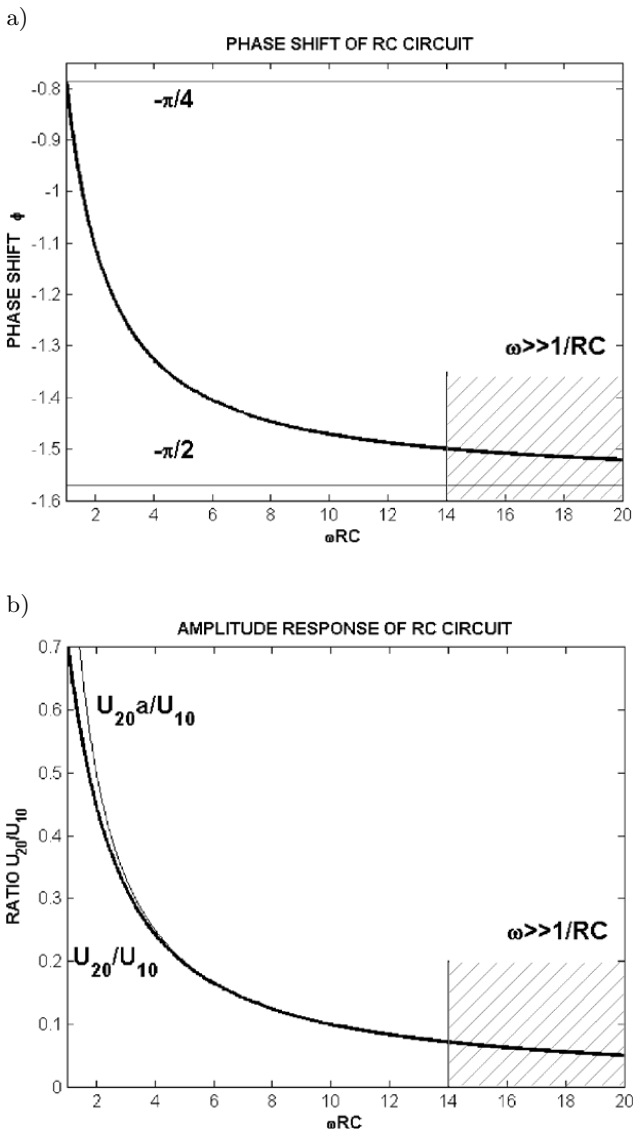
a)

b)

Fig. 4. Transformation of a displacement into a phase-shifted signal by means of integrating an RC circuit.

Transformation of displacement signal into a phase-shifted signal can be realized by a simple active feedback control loop based on the RC circuits consisting of a series of connections of a resistor R and capacitor C.

As a displacement of a harmonic sinusoidal motion $x(t) \approx \sin(\omega t)$ and its velocity $\dot{x}(t) \approx \cos(\omega t) = \sin(\omega t + \pi/2)$ or $\dot{x}(t) \approx \cos(\omega t) = -\sin(\omega t - \pi/2)$ differ by phase shift $\pi/2$, the damping properties of a feedback loop can be based on the utilization of phase shifts realized either by an integrating or by a derivative circuit RC. Since this phase shift is not exact $\pi/2$ but depends on the ratio of angular velocity ω of motion to $1/RC$, i.e. on dimensionless value ωRC, the parameters R, C of a feedback loop must be selected according to the mechanical system.

A sinusoidal input voltage $U_1 = U_{10}\sin(\omega t)$ leads into integrating circuit RC that again produces sinusoidal output $U_2 = U_{20}\sin(\omega t + \psi)$ with amplitude $U_{20} = U_{10}/\sqrt{1+(\omega RC)^2}$ and with a phase angle

$$\psi = \arctan(-\omega RC). \qquad (5)$$

The relationship between ratio U_{20}/U_{10} and dimensionless frequency ωRC is shown in Fig. 4a by a thick line. Phase angle between the output and input of an integrating circuit is shown in Fig. 4b in an interval $-\pi/4 > \psi > -\pi/2$. Phase-shift limits to $-\pi/2$ in the so called "quasi-integration zone" $\omega \gg 1/RC$, is shown, e.g. in Fig. 4, as hatched areas. Amplitudes U_{20} of output voltage are in this zone very low, approximately $U_{20} \cong U_{10}\dfrac{1}{\omega RC}$.
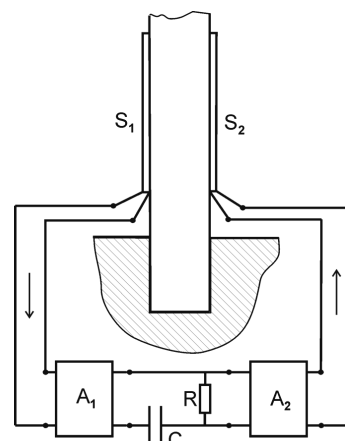

Fig. 5. Scheme of active damping.

The positive phase shift $\pi/2 > \psi > 0$ can also be gained by using a derivative circuit RC but the condition for a quasi-correct value $\psi \approx \pi/2$ is now $0 < \omega \ll 1/RC$ (a quasi-derivation zone). The output signal (ratio U_{20}/U_{10}) is in both cases very low and the signal always has to be amplified.

The application of a derivative circuit RC to increase the damping level in the mechanical system can be shown on the example of a prismatic model of a tur-

bine blade excited by a harmonic force $F_0 \cos(\omega t)$ acting on the free end. Two piezoelectric film sensors are glued near the root of the blade (Fig. 5). The sensor S1 picks up the deformation which is proportional to the deformation of the blade. The output voltage

$$U_1 = U_{10} \sin(\omega t + \psi_1) = k_1 x \qquad (6)_1$$

is lead on the input of high impedance amplifier A_1 connected with RC circuit. Voltage on resistance R

$$U_2 = U_{20} \sin(\omega t + \psi_2) \qquad (6)_2$$

is again amplified in A_2 and leads on the second piezoelectric film sensors S2 which works as an actuator. A suitable selection of RC circuit parameters and amplification of A1, A2 amplifiers makes phase shift between signals U_1 and U_2

$$\Delta \psi = \psi_2 - \psi_1 \cong \pm \pi/2. \qquad (7)$$

Existence of phase shift $\Delta \psi \cong +\pi/2$ enables to write

$$U_2 = U_{20} \sin(\omega t + \psi_1 + \pi/2) = U_{20} \cos(\omega t + \psi_1) \quad (8)$$

and thus, to realize the signal proportional to the velocity and to use it to increase the damping level and to suppress the undesirable dangerous vibrations.

In the numerical model, the additional damping force $b_c \dot{x}$ is proportional to the output voltage U_2

$$b_c \dot{x} = k_{fb} U_2, \qquad (9)$$

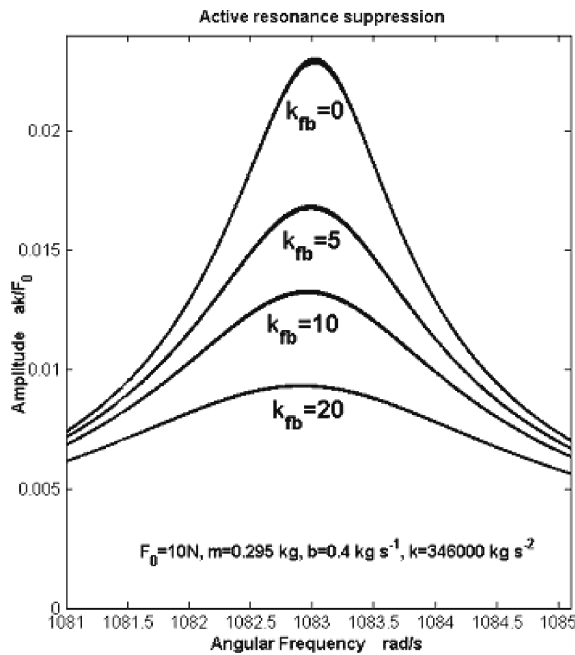where the constant k_{fb} is a function of the parameters of piezoelectric film sensors S1, S2, amplifying constants of amplifiers A1, A2 and transfer function of RC circuit.

Influence of k_{fb} of the entire feedback loop on reduction of resonance amplitudes of clamped beam is shown in Fig. 6, where the mechanical system has the same dimensions and frequency spectrum as the blade described in Sec. 3. The parameters of a derivative RC circuit, modeled by the differential equation of the 1st order, were R = 10 Ω, C = 0.01 C. It is evident that considerable suppression of undesired resonance vibrations can be reached by the means of active feedback loops with piezoelectric films connected as sensors and actuators.

5. Description and results of the dynamic experiments

Tests of the PVDF film actuators were based on the excitation of the first flexural resonant vibration of the clamped beam with the registration of its dynamic responses (Fig. 7). The prismatic steel blade has a rectangular cross-section with the following dimensions: height 10 mm : width 18 mm : length 240 mm. The free length of the clamped beam is 210 mm. Two strips of PVDF film (DT2-028K/L, 28 μm : 12 mm : 62 mm) were glued, each of them on the opposite sides of the beam near (range 25–87 mm) the clamping. Since the PVDF strips (total capacity 5 nF) were connected anti-parallelly in the circuit, they act together in the same phase similarly as a model with a single layer (Fig. 1). Besides PVDF actuators, an electromagnet as a reference actuator was installed in the vicinity (clearance space 1 mm) to the blade tip. The dynamic force (F_{em}) of the electromagnet was measured by the force transducer Deltatron B&K8200. The movement of the blade was picked up by the miniature accelerometers B&K4734 placed at the end (AL_1) and in the middle of the blade length (AL_2). The amplifiers of both

Fig. 6. Suppression of resonance peak by means of active feedback loop, according to the scheme in Fig. 5.
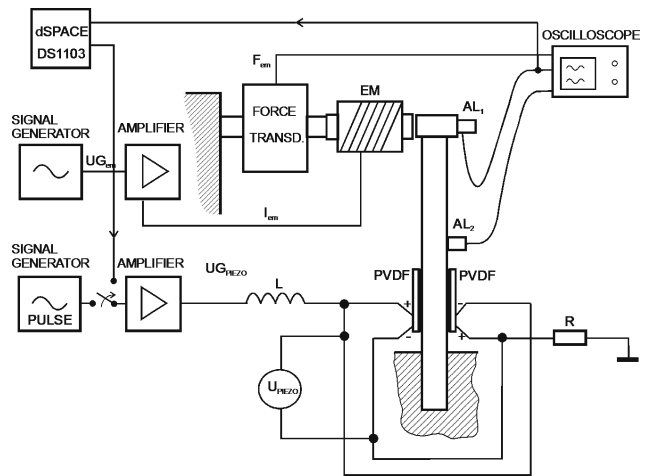
Fig. 7. Set up of the experiment for a feedforward and feedback control.

electromagnet and the PVDF films were excited by signals of the generators (UG$_{em}$, UG$_{piezo}$) of the system PULSE B&K 14.0. Series connection of the inductance ($L = 30$ H) in the circuit with PVDF strips compensates a small value of their capacitance that acts as high resistance of the alternate current of frequencies about 170 Hz. Series connection of the resistance brings into the circuit certain damping that widens the electric resonance peak and enables to overlap the mechanical and electrical resonance peaks. The force (F_{em}), accelerometer signals (AL$_1$, AL$_2$), the output voltages of the generators (UG$_{em}$, UG$_{piezo}$), the supply current of electromagnet (I$_{em}$), and the supply voltage of the strips (U$_{piezo}$) were registered by a digital oscilloscope.

The experiment was divided into several stages. In the first stage, we evaluated the excitation effect and the mechanical power of PVDF strips on the forced resonant vibration (168.45 Hz) of the beam with respect to the supply voltages $U = 90$ V and 120 V. The maximal achieved levels of accelerations AL$_1$ (24.2 ms^{-2}) of the beam excited by the strips helped us in this stage to a) set the corresponding supply current of the electromagnet for testing the feasibility of the strips to amplify or suppress the electromagnetic forced resonant vibrations of the beam. In this stage of a feedforward control, we analysed the influence of the phase shift between the electromagnet and PVDF strips on the forced resonant vibration excited by the low level electromagnetic force equivalent to the piezo foil excitation power. The excitation frequency of the strips was set slightly different

at 168.455 Hz than of the electromagnet at 168.45 Hz in the third stage of the experiment. This slightly unbalanced frequencies of the harmonic signals cause a mutual phase shift in the interval $(0, 360)°$ with a period of beats 200 s. In the last stages b), c) of the feedback control, we aimed at the verification of the numerical results of the parametric excitation and active damping suppression effects. Due to the low mechanical power of the PVDFs, the analysis of the additional parametric excitation and the active damping was performed at lower levels of electromagnetic excitation.

5.1. Forced resonant vibration exited by electromagnet – phase-angle setup of piezoactuation

The time characteristics of the selected measured signals U$_{piezo}$, F$_{em}$ and AL$_1$ are presented in Fig. 8. The zooms of these characteristics when amplitudes AL$_1$ reach their maximal and minimal values are shown in Fig. 9. As can be seen in these figures, the amplitude amplifying effect occurred when the strips acted in phase to the electromagnetic excitation. The minimum amplitudes arose at the times when the moment of the strips acts in anti-phase to the electromagnetic excitation. Since in the resonance of the beam the electromagnetic force is in the phase with the velocity of the beam vibration, the maximal vibrational amplification and suppression effect of the strips is achieved by the in-phase or anti-phase, respectively, synchronization of their force actuation with the velocity.
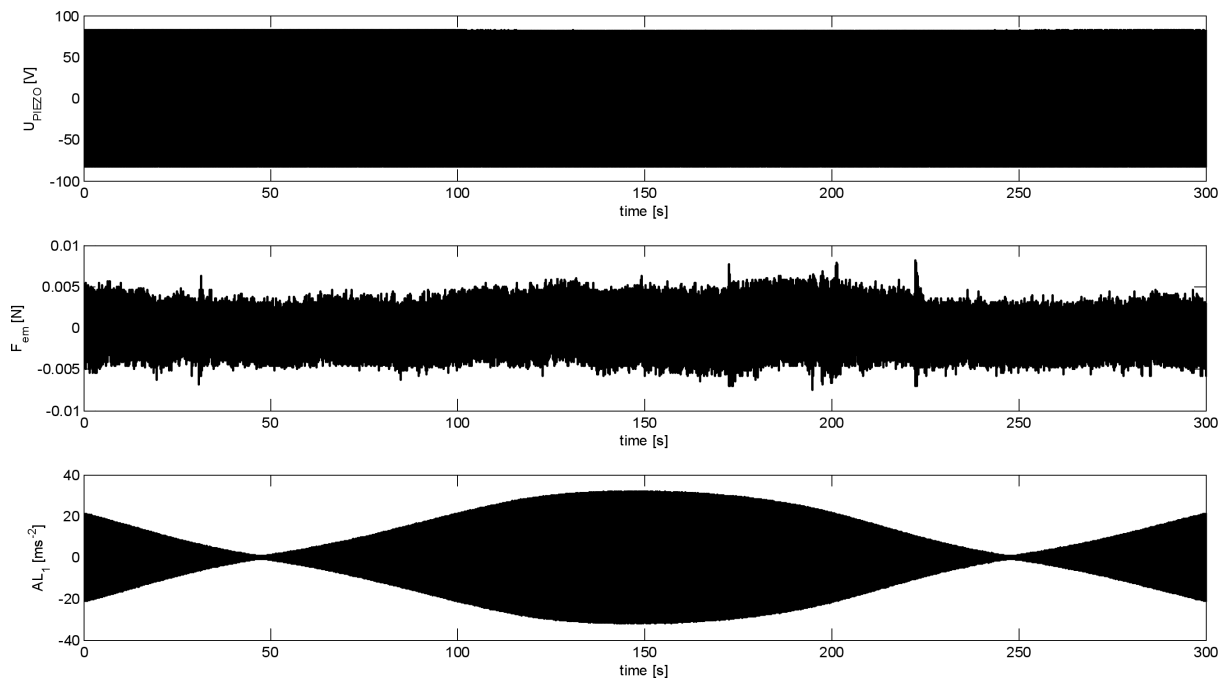

Fig. 8. The time characteristics of supply voltage of the strips (U$_{piezo}$), electromagnetic force (F$_{em}$) and beam end acceleration (AL$_1$) – forced resonant vibration with piezoactuation in the open loop.
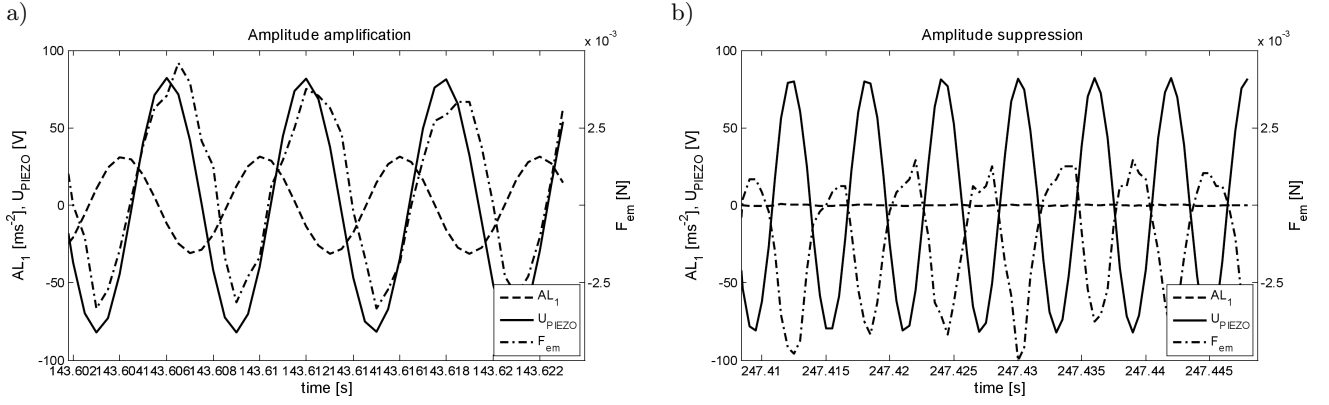
a)

b)

Fig. 9. The zoomed time characteristics of supply voltage of the strips (U_{piezo}), electromagnetic force (F_{em}) and beam end acceleration (AL_1) in a case of: a) vibration amplification, b) vibration suppression – forced resonant vibration with piezoactuation in the open loop.

5.2. Forced resonant vibration excited by electromagnet – piezoactuation as additional parametric excitation

The experimental set-up was modified for the realization of the additional parametric excitation. Instead of the PULSE generation of UG_{piezo} signal, the control system dSPACE 2013-B with the unit DS1103 was switched to the feedback control (see Fig. 7). Control programs of the unit DS1103 were created in the Matlab-SIMULINK environment. Contrary to the mathematical model, the time variable elastic force $\varepsilon \mathbf{K_p} \cos(\nu t)\mathbf{y}(t)$ in the Eq. (2) was substituted by the piezofilm moment (M_p) supplied by the synthesized voltage signal $U_{piezo} = k_a \cos(\nu t)y_s(t)$, where y_s is a scaled displacement and k_a is amplification factor (Fig. 10). A similar concept of the feedback was pre-

sented by (TŮMA *et al.*, 2014). Since the suppression of the harmonic resonant vibration was assumed, we used the measured signal AL_1 of accelerometer with an opposite sign as displacement input y_s in our control algorithm. The angular frequency ν was set to 5515.4 rad/s since experimental values of eigenfrequencies were $\Omega_1 = 1058.1$, $\Omega_2 = 6573.5$ rad/s.
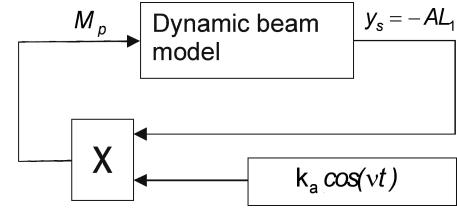

Fig. 10. Block diagram of the feedback loop for piezoactuation as additional parametric excitation.
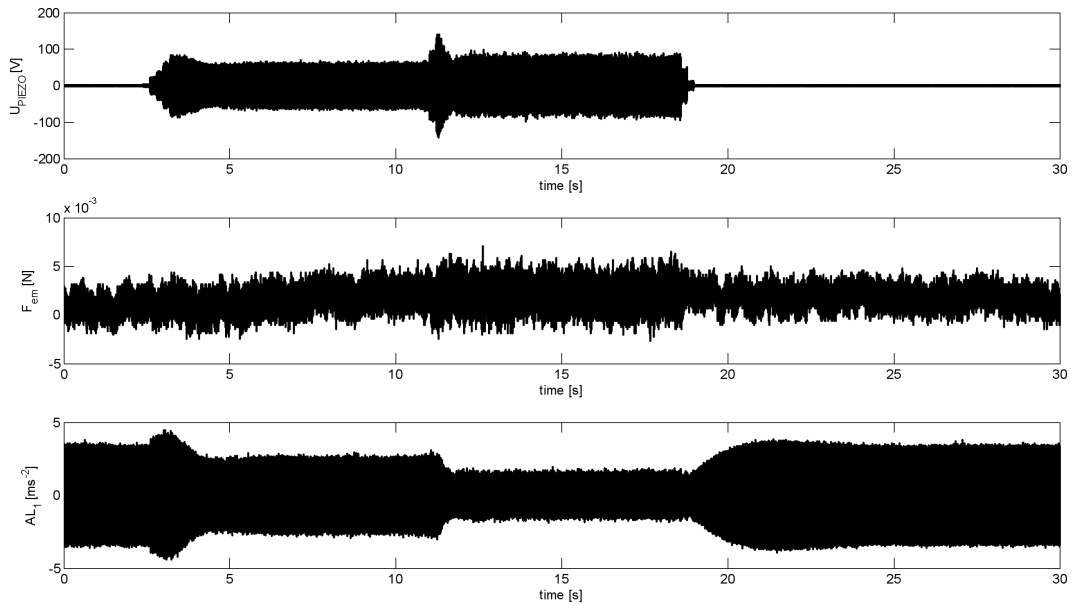

Fig. 11. The time characteristics of supply voltage of the strips (U_{piezo}), electromagnetic force (F_{em}) and beam end acceleration (AL_1) with/without additional parametric excitation.
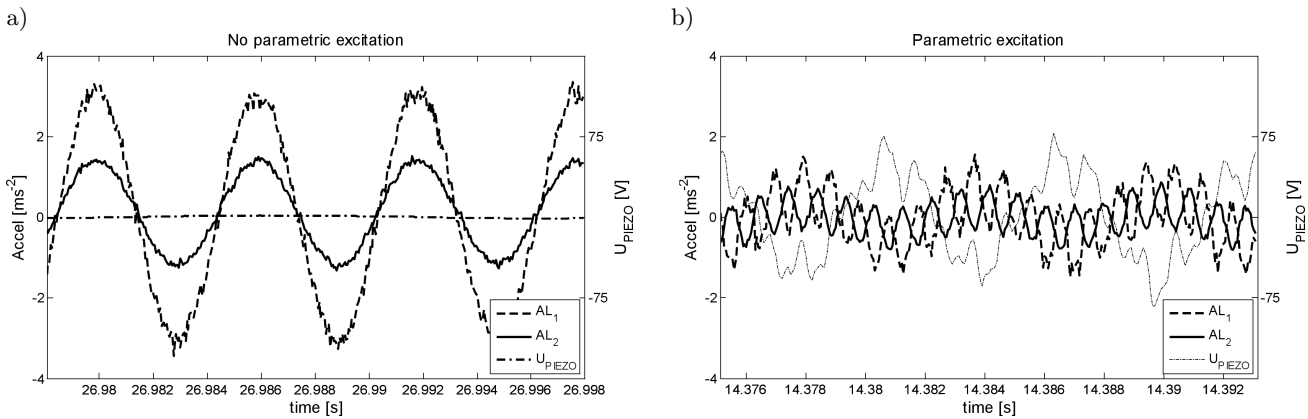
a)

b)

Fig. 12. The zoomed time characteristics of supply voltage of the strips (U_{piezo}) and beam accelerations (AL_1, AL_2) in a case of: a) no additional parametric excitation, b) with additional parametric excitation.

The results of this test are summarized in the next figures. The time characteristics of the selected measured signals U_{piezo}, F_{em} and AL_1 without (intervals (0–3)s, (19–30)s) and with additional parametric excitation (lower level (3–11)s, higher level (12–19)s) are presented in Fig. 11. The zooms of two intervals for without and with parametric excitation are shown in Fig. 12. When comparing the amplitudes of AL_1 in Figs. 11 and 12, we can see a strong suppression effect of the blade vibration due to the parametric excitation. The character of vibration, i.e. modulation of the force excited displacements by the second resonant frequency during the additional parametric excitation, is in accordance with the theoretical findings presented in Chapter 3.

5.3. Forced resonant vibration excited by electromagnet – piezoactuation as active damping

The same experimental set-up with the unit DS1103 of the control system dSPACE 2013-B was used. The active damping described in Chapter 4 was realized by the bending moment (M_p) of the piezofilm supplied by the synthesized voltage signal $U_{piezo} = k_a \dot{y}_s(t)$, where $\dot{y}_s$ represents a scaled velocity and k_a
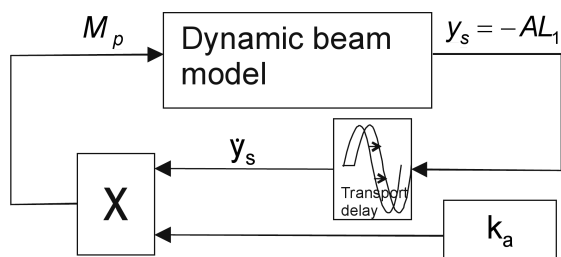
is an amplification factor (Fig. 13). A control program was created again in the Matlab-SIMULINK. Assuming the harmonic displacement at the resonant vibration, we used the $\pi/2$ phase-shifted signal of AL_1 as the velocity input in our control algorithm. The phase shift was realized by the transport delay Simulink block.

To evaluate the suppression effect, two types of dynamic loadings were used a) harmonic resonant excitation (168.45 Hz) (Figs. 14, 15), and b) sweep excitation over the first resonance 166.5–170.5 Hz, swept time 30 s (Figs. 16, 17).

a) The time characteristics of the selected measured signals U_{piezo}, F_{em} and AL_1 are shown in Fig. 14. The different levels of voltage supply U_{piezo} were applied during the forced resonant vibrations driven by the electromagnetic force F_{em}. The response of the blade can be observed on the signal AL_1. It can be seen that the suppression of vibrations is linearly dependent on the level of the supply. At the highest level, the vibrations are almost completely suppressed, as it is shown in Fig. 15. For comparison, the next zoom of Fig. 15 shows the signals at switched off the active damping.

b) The effect of the active damping based on the velocity feedback at the sweep harmonic excitation is shown in Fig. 16. The three sweep overruns of the first resonance are recorded herein. The active damping was switched only during the second overrun. The detailed characteristics and the decrease of the vibration amplitudes almost by half can be seen on the zooms in Fig. 17. The lower decrease of amplitudes than in the previous case can be explained by transient excitation conditions and the stabilization time of the feedback needed for an optimal suppression.
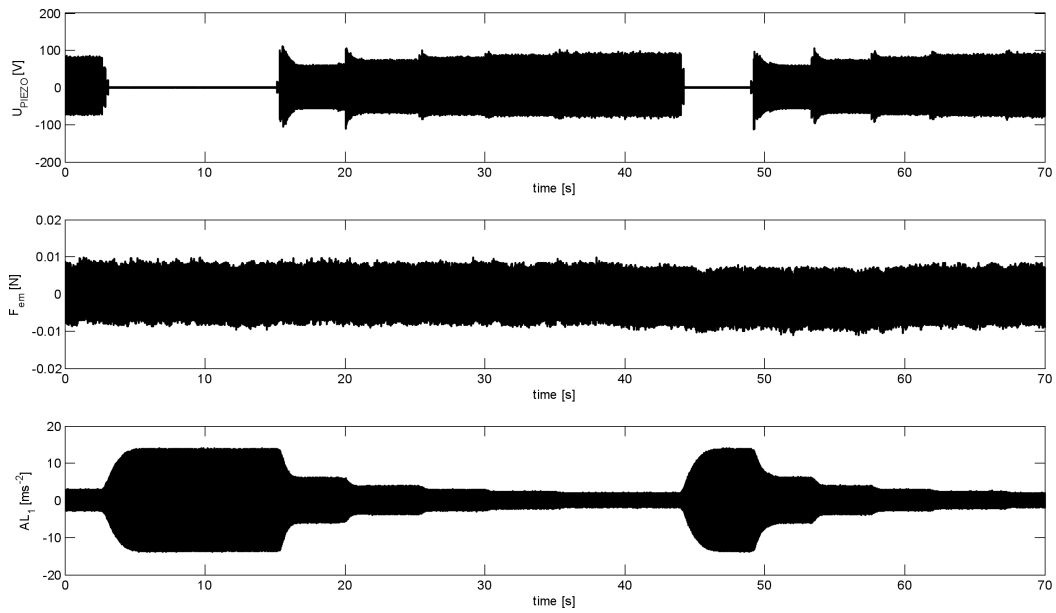

Fig. 13. Block diagram of the feedback loop for piezoactuation as active damping.

Fig. 14. The time characteristics of supply voltage of the strips (U_{piezo}), electromagnetic force (F_{em}) and beam end acceleration (AL_1) with/without active damping – harmonic resonant vibration.
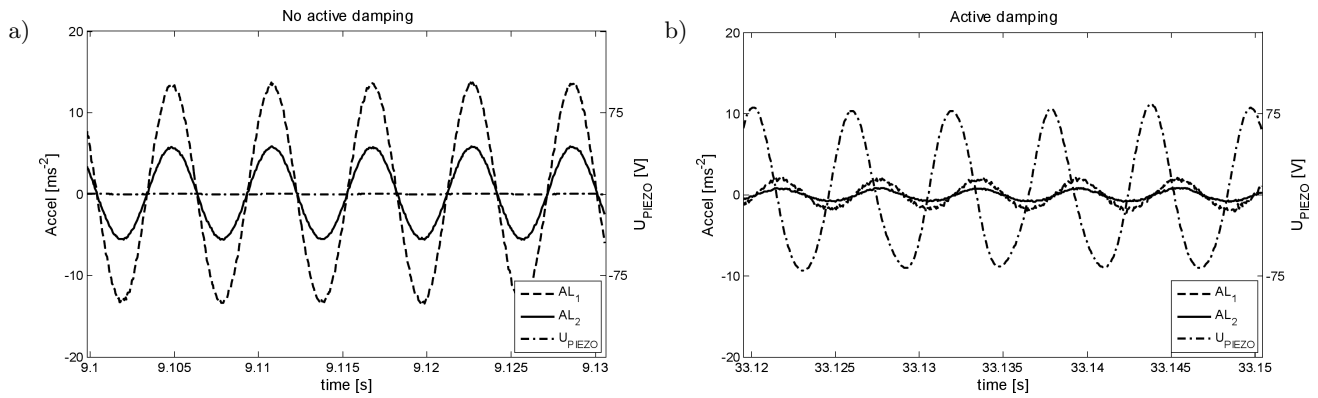

Fig. 15. The zoomed time characteristics of supply voltage of the strips (U_{piezo}) and beam accelerations (AL_1, AL_2) in a case of: a) no active damping, b) active damping – harmonic resonant vibration.
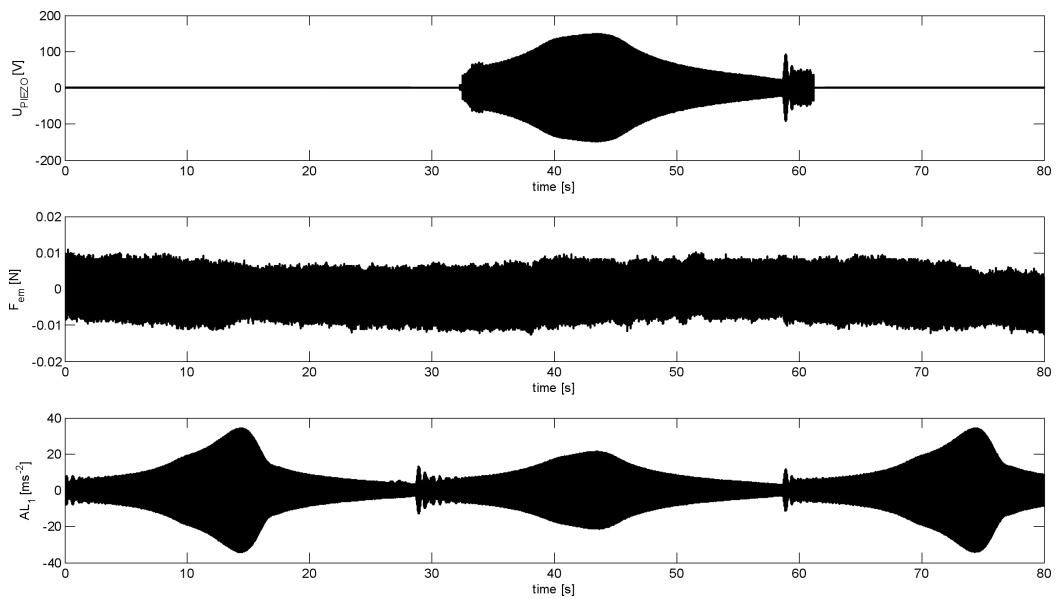

Fig. 16. The time characteristics of supply voltage of the strips (U_{piezo}), electromagnetic force (F_{em}) and beam end acceleration (AL_1) with/without active damping – sweep excitation.
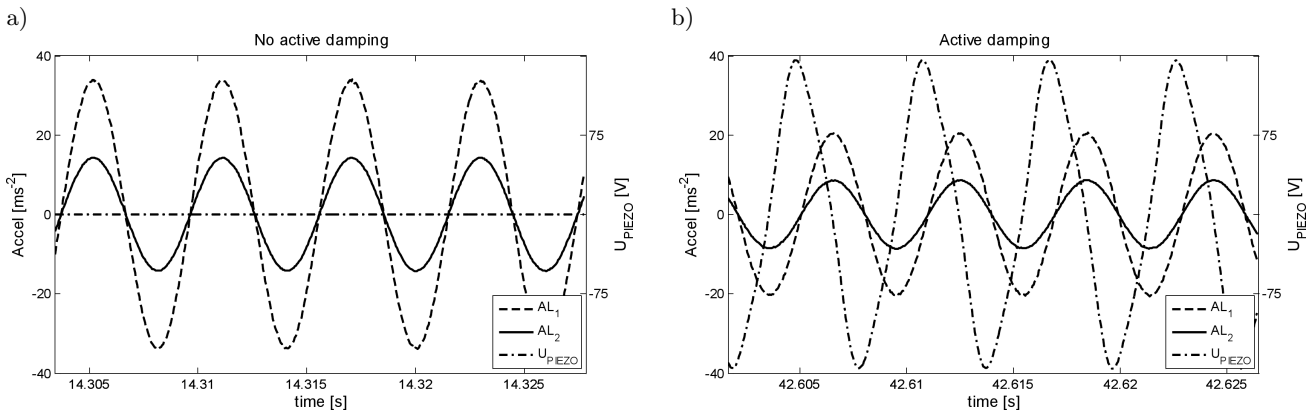
Fig. 17. The zoomed time characteristics of supply voltage of the strips (U_{piezo}) and beam acceleration (AL_1, AL_2) in a case of: a) no active damping, b) active damping – sweep excitation.

6. Conclusion

Dynamical tests of the PVDF films on the active control of flexural vibration of the blade model confirmed the theoretical levels of bending moments at given levels of a supply voltage measured on the piezoelectric electrodes. The force actuation of the films was then introduced into the numerical model of the blade to analyse the vibration suppression effects both by additional parametric excitation and by the active damping. Numerical results of both approaches predicted a strong amplitude attenuation. The suppression vibration effect was confirmed by the experiments.

Since the vibration levels evoked by the by PVDF excitation were tens of microns, the low level of electromagnetic excitation was used to ascertain the optimal phase angles of the PVDF excitation with respect to the blade vibration movement both for maximal vibration amplification and suppression. The values of optimal phases showed that the beam resonant vibration can be easily amplified or suppressed by in-phase or anti-phase, respectively, synchronization of PVDF films with the beam velocity.

For real applications of laboratory tests of turbine blades, the excitation capacity of the piezoelectric elements should be high enough to evoke vibrations about several millimeters at the blade tips. Higher excitation effect can be assumed at the PZT patches at which the blocking forces result two order higher than at the PVDF films. Therefore in the next study, the achieved results will be used to the application of the PZT patches for actuation and to actively control blade vibrations.

Acknowledgments

References

1. AUGUSTYN E., KOZIEN M.S. (2014), *A Study on Possibility to Apply Piezoelectric Actuators for Active Reduction of Torsional Beams Vibrations*, Acta Physica Polonica, **125**, 4A, A164–A168.

2. BELL A.J. (1993), *Multilayer ceramic processing*, Ferroelectric Ceramics, Birkhäuser Verlag, Basel, 241–271.

3. JARZYNA W., AUGUSTYNIAK M., BOCHENSKI M., WARMINSKI J. (2012), *PD and LQR controllers applied to vibration damping of an active composite beam*, Przeglad Elektrotechniczny, **88**, 10B, 128–131.

4. NADER M., BERGER W. (2013), *Applications of piezoelectric patches for active noise and vibration reduction or generation*, Proceedings of 6th ECCOMAS Conference on Smart Structures and Materials, 11 pages, 2013, Turin.

5. NORDMAN R. (2005), *Mechatronic systems in Machinery I*, [in German: *Mechatronische Systeme im Maschinenbau I.*], Shaker-Verlag, Darmstadt.

6. PEŠEK L., HAJŽMAN M., PŮST L., ZEMAN V., BYSTUS M., BRŮHA J. (2014a), *Experimental and numerical investigation of friction element dissipative effects in blade shrouding*, Journal of Nonlinear Dynamics, Springer, published on-line, 12 pages, DOI: 10.1007/s11071-014-1763-3.

7. PEŠEK L., PŮST L., BULA V., VANĚK F. (2012), *Interslip damping of twisted blades in opposed bundles under rotation*, Proceedings of 10th International Conference on Vibrations in Rotating Machinery, Woodhead Publishing Limited Book, pp. 293–302, London.

8. PEŠEK L., VANĚK FR., PŮST L., BULA L, CIBULKA J. (2010), *Testing of dynamics of blade wheel with double periodicity*, Engineering Mechanics, **17**, 3/4, 237–250.

9. PEŠEK L., VANĚK F., BULA V., CIBULKA J. (2011), *Excitation of blade vibration under rotation by synchronous electromagnet*, Engineering Mechanics, **18**, 3/4, 1–9.

10. PEŠEK L., TONDL A. (2012), *Contribution to application of parametric 'anti-resonance' for autoparametric systems*, Egineering Mechanics, **19**, 5, 1–9.

11. Pešek L., Půst L, Bula V., Cibulka J. (2014b) *Testing of piezofilms for actuation and active control of blade flexural vibration*, Proceedings of 7th EAA Conference on Forum Acusticum, 12 pages, Krakow.

12. Preumont A. (2011), *Vibration Control of Active Structures*, Springer-Verlag, Berlin.

13. Půst L., Pešek L. (2011), *Vibration of circular bladed disk with imperfections*, International Journal of Bifurcation and Chaos, **21**, 10, 2893–2904.

14. Rybak L.A. *et al.* (1997), *Synthesis of active systems of vibroisolations on space objects*, [in Russian: *Sintez aktivnych sistem vibroizolacii na kosmiceskich objektach*], Janus-K, Moscow.

15. Tondl A., Půst L. (2012), *On the phenomenon "Parametric anti-resonnce"*, Strojnický časopis, **63**, 3, 125–137.

16. Tondl A. (1998), *Vibration quenching of an externally excited system by means of dynamic absorber*, Acta Technica CSAV, **43**, 301–309.

17. Tůma J., Šuránek P., Mahdal M. (2014), *Simulation study on the forced response of the non-stationary second order system*, Proceedings of 21th Colloquium Dynamics of Machines 2014, IT AS CR, pp. 171–177, Prague.

18. Warminski J., Bochenski M., Jarzyna W., Filipek P., Augustyniak M. (2011), *Active suppression of nonlinear composite beam vibrations by selected control algorithms*, Communications in Nonlinear Science and Numerical Simulation, **16**, 5, 2237–2248.

19. Warminski J., Cartmell M.P., Mitura A., Bochenski M. (2013), *Active vibration control of a nonlinear beam with self- and external excitations*, Shock and Vibration, **20**, 1033–1047.